PERGAMON

International Journal of Solids and Structures 39 (2002) 5753–5765

INTERNATIONAL JOURNAL OF SOLIDS and STRUCTURES

www.elsevier.com/locate/ijsolstr

Analysis of a transversely isotropic rod containing a single cylindrical inclusion with axisymmetric eigenstrains

Z. Zhong [a,*], Q.P. Sun [b]

[a] *Solid Mechanics Key Laboratory of MOE, Department of Engineering Mechanics and Technology, Tongji University, Shanghai 200092, China*

[b] *Department of Mechanical Engineering, The Hong Kong University of Science and Technology, Clear Water Bay, Kowloon, Hong Kong SAR, China*

Received 16 January 2002; received in revised form 7 August 2002

Abstract

This paper studies a transversely isotropic rod containing a single cylindrical inclusion with axisymmetric eigenstrains. The analytical elastic solution is obtained for the displacements, stresses and elastic strain energy of the rod. The effects of microstructural parameters and its evolution on the elastic stress and strain fields as well as the strain energy of the rod are quantitatively demonstrated through examples.

Keywords: Transversely isotropic rod; Cylindrical inclusion; Axisymmetric eigenstrain

1. Introduction

Experimental observations on tensile test of NiTi polycrystalline shape memory alloy wires and strips have shown that the deformation in the superelastic region is realized by the reversible propagation of single band and multi-bands during the forward and reverse transformations (Leo et al., 1993; Lin et al., 1994; Shaw and Kyriakides, 1995, 1997). These phenomena motivated the study of a new type of inclusion-matrix system: an infinite circular cylindrical rod containing a single inclusion with uniform axisymmetric eigenstrains (Zhong et al., 2000). This kind of inclusion problem is different from the traditional Eshelby-type inclusion problems (Eshelby, 1957; Mura, 1987; among others) in that the inclusion is not fully bounded by the matrix. The solution of such a new inclusion problem has been employed to predict the force–displacement relationship in the uniaxial tensile loading of the SMA wire specimen under isothermal or very slow loading rate cases (Sun and Zhong, 2000).

In our previous paper (Zhong et al., 2000), the assumption of isotropy was made for the elastic properties of the rod, while in the present paper we considered a more general case of transversely isotropic rod

* Corresponding author. Tel.: +86-21-65982483.
E-mail address: zhongk@online.sh.cn (Z. Zhong).

0020-7683/02/$ - see front matter
PII: S0020-7683(02)00459-6

containing a single cylindrical inclusion with uniform axisymmetric eigenstrains which may apply to crystallographically textured SMA rods. An analytical solution for the displacements, stresses and elastic strain energy of the rod is obtained. In Section 2, the basic equations and boundary conditions for the problem are described. In Section 3, solution techniques to determine the stress and displacement fields as well as the strain energy of the rod are formulated. The results are discussed through examples in Section 4, and finally a summary is given in Section 5.

2. Problem statement and basic equations

Consider an infinite long cylindrical rod with a circular cross section of radius a which contains a uniform axisymmetric eigenstrain ε_{ij}^* (induced by phase transformation or other sources) in a cylindrical inclusion of height l, as shown in Fig. 1. A cylindrical coordinate system (r, θ, z) is introduced with the z-axis placed along the axis of revolution of the cylinder. The elastic properties of the rod are assumed to be transversely isotropic with the axial direction of symmetry coinciding with the z-axis. The elastic constants of the inclusion are the same as the remaining matrix (Note: in real martensitic transformation in SMA, the Young's modulus of martensite is less than that of austenite, then it will be treated as an inhomogeneous inclusion problem). The uniform axisymmetric eigenstrain ε_{ij}^* will cause nonuniform deformation and internal stress in the rod and its nonzero components can be given as

$$\varepsilon_r^* = \varepsilon_\theta^* = \varepsilon_1^* \quad \varepsilon_z^* = \varepsilon_2^* \tag{1}$$

The corresponding displacement components are denoted by u_r, u_θ, u_z, the component u_θ vanishes and u_r, u_z are independent of θ. The nonzero strain components ε_r, ε_θ, ε_z and γ_{rz} are calculated by the following strain-displacement relations:

$$\varepsilon_r = \frac{\partial u_r}{\partial r} \quad \varepsilon_\theta = \frac{u_r}{r} \quad \varepsilon_z = \frac{\partial u_z}{\partial z} \quad \gamma_{rz} = \frac{\partial u_r}{\partial z} + \frac{\partial u_z}{\partial r} \tag{2}$$

The corresponding stress components σ_r, σ_θ, σ_z and τ_{rz} in the inclusion $(|z| < l/2, r < a)$ can be obtained as

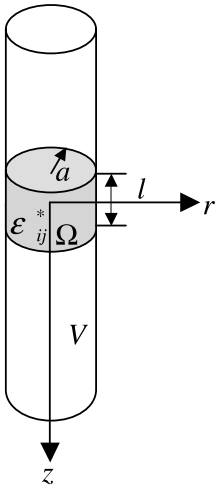

Fig. 1. A schematic of a cylindrical rod with an inclusion.

$$\begin{aligned}
\sigma_r &= c_{11}(\varepsilon_r - \varepsilon_r^*) + c_{12}(\varepsilon_\theta - \varepsilon_\theta^*) + c_{13}(\varepsilon_z - \varepsilon_z^*)\\
\sigma_\theta &= c_{12}(\varepsilon_r - \varepsilon_r^*) + c_{11}(\varepsilon_\theta - \varepsilon_\theta^*) + c_{13}(\varepsilon_z - \varepsilon_z^*)\\
\sigma_z &= c_{13}(\varepsilon_r - \varepsilon_r^*) + c_{13}(\varepsilon_\theta - \varepsilon_\theta^*) + c_{33}(\varepsilon_z - \varepsilon_z^*)\\
\sigma_{rz} &= c_{44}\gamma_{rz}
\end{aligned} \tag{3}$$

while their counterparts in the matrix ($|z| > l/2, r < a$) are obtained as

$$\begin{aligned}
\sigma_r &= c_{11}\varepsilon_r + c_{12}\varepsilon_\theta + c_{13}\varepsilon_z\\
\sigma_\theta &= c_{12}\varepsilon_r + c_{11}\varepsilon_\theta + c_{13}\varepsilon_z\\
\sigma_z &= c_{13}\varepsilon_r + c_{13}\varepsilon_\theta + c_{33}\varepsilon_z\\
\sigma_{rz} &= c_{44}\gamma_{rz}
\end{aligned} \tag{4}$$

where c_{11}, c_{12}, c_{13}, c_{33} and c_{44} are elastic constants of the transversely isotropic rod.

The stress components either in the inclusion or in the matrix should satisfy the equations of equilibrium as follows:

$$\begin{aligned}
&\frac{\partial\sigma_r}{\partial r} + \frac{\partial\sigma_{rz}}{\partial z} + \frac{\sigma_r - \sigma_\theta}{r} = 0\\
&\frac{\partial\sigma_{rz}}{\partial r} + \frac{\partial\sigma_z}{\partial z} + \frac{\sigma_{rz}}{r} = 0
\end{aligned} \tag{5}$$

Substituting (2)–(4) into (5), we obtain the governing equations for the displacements either in the inclusion or in the matrix:

$$\begin{aligned}
&(c_{13} + c_{44})\frac{\partial\Theta}{\partial r} + (c_{11} - c_{13} - c_{44})\left(\nabla^2 u_r - \frac{u_r}{r^2}\right) - (c_{11} - c_{13} - 2c_{44})\frac{\partial^2 u_r}{\partial z^2} = 0\\
&(c_{13} + c_{44})\frac{\partial\Theta}{\partial z} + c_{44}\nabla^2 u_z + (c_{33} - c_{13} - 2c_{44})\frac{\partial^2 u_z}{\partial z^2} = 0
\end{aligned} \tag{6}$$

where $\nabla^2 = \partial^2/\partial r^2 + (1/r)\partial/\partial r + \partial^2/\partial z^2$, $\Theta = \varepsilon_r + \varepsilon_\theta + \varepsilon_z$.

The boundary conditions for the lateral surface ($r = a$) can be written as

$$\sigma_r = \sigma_{rz} = 0 \quad (r = a) \tag{7}$$

which means no force is applied at the lateral surface. The continuity conditions for the traction and displacement at the planar interface between the inclusion and the matrix require that the displacements u_r, u_z and the stresses σ_z, σ_{rz} be continuous at the interface $z = l/2$ and $z = -l/2$. The stress-free end condition of the infinite cylindrical rod can be written as

$$\sigma_r = \sigma_{rz} = 0 \quad (|z| \to \infty) \tag{8}$$

In the following sections, the deformation and stress field in the rod will be determined using the above basic equations and boundary conditions.

3. Solution

3.1. Decomposition of the problem

The solution of the above original problem is the superposition of the solutions of the following two sub-problems:

$$u_r = u_r^{\mathrm{I}} + u_r^{\mathrm{II}} \quad u_z = u_z^{\mathrm{I}} + u_z^{\mathrm{II}}$$
$$\sigma_r = \sigma_r^{\mathrm{I}} + \sigma_r^{\mathrm{II}} \quad \sigma_\theta = \sigma_\theta^{\mathrm{I}} + \sigma_\theta^{\mathrm{II}} \tag{9}$$
$$\sigma_z = \sigma_z^{\mathrm{I}} + \sigma_z^{\mathrm{II}} \quad \sigma_{rz} = \sigma_{rz}^{\mathrm{I}} + \sigma_{rz}^{\mathrm{II}}$$

3.1.1. Sub-problem I

The displacements of the rod are assumed to have the following forms:

$$u_r^{\mathrm{I}} = 0 \quad u_z^{\mathrm{I}} = \Gamma z \quad \left(|z| < \frac{l}{2}, r < a\right)$$
$$u_r^{\mathrm{I}} = 0 \quad u_z^{\mathrm{I}} = -\Gamma\frac{l}{2} \quad \left(z < -\frac{l}{2}, r < a\right) \tag{10}$$
$$u_r^{\mathrm{I}} = 0 \quad u_z^{\mathrm{I}} = \Gamma\frac{l}{2} \quad \left(z > \frac{l}{2}, r < a\right)$$

with

$$\Gamma = \frac{2c_{13}}{c_{33}}\varepsilon_1^* + \varepsilon_2^* \tag{11}$$

The corresponding stresses in the rod are obtained as

$$\sigma_r^{\mathrm{I}} = \sigma_\theta^{\mathrm{I}} = -\left(c_{11} + c_{12} - \frac{2c_{13}^2}{c_{33}}\right)\varepsilon_1^* \quad \sigma_z^{\mathrm{I}} = \sigma_{rz}^{\mathrm{I}} = 0 \quad \left(|z| < \frac{l}{2}, r < a\right)$$
$$\sigma_r^{\mathrm{I}} = \sigma_\theta^{\mathrm{I}} = \sigma_z^{\mathrm{I}} = \sigma_{rz}^{\mathrm{I}} = 0 \quad \left(|z| > \frac{l}{2}, r < a\right) \tag{12}$$

The assumed solution of displacements in (10) automatically satisfies the governing equation (6) and the remote end condition (8) as well as the continuity conditions for the traction and displacement at the interface between the inclusion and the matrix. Unfortunately, the lateral boundary condition (7) is not satisfied. At the boundary $r = a$, the solution gives

$$\sigma_r^{\mathrm{I}} = -\left(c_{11} + c_{12} - \frac{2c_{13}^2}{c_{33}}\right)\varepsilon_1^* \quad \sigma_{rz}^{\mathrm{I}} = 0 \quad \left(|z| < \frac{l}{2}, r = a\right)$$
$$\sigma_r^{\mathrm{I}} = \sigma_{rz}^{\mathrm{I}} = 0 \quad \left(|z| > \frac{l}{2}, r = a\right) \tag{13}$$

In order to satisfy boundary condition (7), an auxiliary solution should be superimposed, which will be described as sub-problem II.

3.1.2. Sub-problem II

The same rod, stress free on its two ends, is subjected to uniformly distributed pressure p over $|z| < l/2$, as shown in Fig. 2. The basic equations and the boundary conditions at the remote ends are the same as Eqs. (2)–(6) and (8) (let $\varepsilon_{ij}^* = 0$), while the lateral boundary condition can be described as

$$\sigma_r^{\mathrm{II}} = -p \quad \sigma_{rz}^{\mathrm{II}} = 0 \quad \left(|z| < \frac{l}{2}, r = a\right)$$
$$\sigma_r^{\mathrm{II}} = \sigma_{rz}^{\mathrm{II}} = 0 \quad \left(|z| > \frac{l}{2}, r = a\right) \tag{14}$$

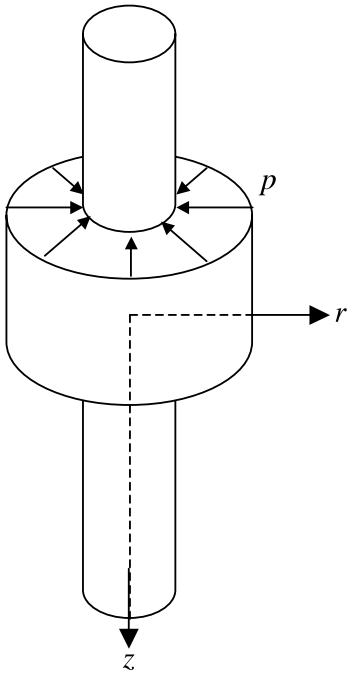

Fig. 2. A schematic of a cylindrical rod subjected to a distributed pressure p.

where

$$p = -\left(c_{11} + c_{12} - \frac{2c_{13}^2}{c_{33}}\right)\varepsilon_1^* \tag{15}$$

To obtain the solution of sub-problem II, a stress function ψ is introduced following the solution technique given in the book by Lekhnitski (1981), such that

$$\begin{aligned} u_r^{\mathrm{II}} &= A\frac{\partial^2\psi}{\partial r\partial z} \\ u_z^{\mathrm{II}} &= \frac{\partial^2\psi}{\partial r^2} + \frac{1}{r}\frac{\partial\psi}{\partial r} + B\frac{\partial^2\psi}{\partial z^2} \end{aligned} \tag{16}$$

where

$$A = -\frac{c_{13} + c_{44}}{c_{11}} \quad B = \frac{c_{44}}{c_{11}} \tag{17}$$

and ψ should satisfy the equation

$$\nabla_1^2\nabla_2^2\psi = 0 \tag{18}$$

Where $\nabla_i^2 = \partial^2/\partial r^2 + (1/r)\partial/\partial r + \lambda_i(\partial^2/\partial z^2)$, $i = 1, 2$; and the constants, λ_1 and λ_2, are given by

$$\lambda_1 = \frac{d + \sqrt{d^2 - 4b}}{2} \quad \lambda_2 = \frac{d - \sqrt{d^2 - 4b}}{2} \tag{19}$$

in which

$$b = \frac{c_{33}}{c_{11}} \quad d = \frac{c_{11}c_{33} - 2c_{13}c_{44} - c_{13}^2}{c_{11}c_{44}} \tag{20}$$

Eq. (18) is obtained by substituting (16) into (6). It can be shown that p_1 and p_2 are either real or complex and they are never purely imaginary (Lekhnitski, 1981). For an isotropic material, we have $c_{11} = c_{33}$, $c_{12} = c_{13}$, $c_{44} = (c_{11} - c_{13})/2$ and $\lambda_1 = \lambda_2 = 1$. In this special case, Eq. (18) reduces to the well-known bi-harmonic equation

$$\nabla^2\nabla^2\psi = 0 \tag{21}$$

Accordingly, the stresses are written as

$$\begin{aligned}
\sigma_r^{\mathrm{II}} &= (c_{11}A + c_{13})\frac{\partial^3\psi}{\partial r^2\partial z} + (c_{12}A + c_{13})\frac{1}{r}\frac{\partial^2\psi}{\partial r\partial z} + c_{13}B\frac{\partial^3\psi}{\partial z^3} \\
\sigma_\theta^{\mathrm{II}} &= (c_{12}A + c_{13})\frac{\partial^3\psi}{\partial r^2\partial z} + (c_{11}A + c_{13})\frac{1}{r}\frac{\partial^2\psi}{\partial r\partial z} + c_{13}B\frac{\partial^3\psi}{\partial z^3} \\
\sigma_z^{\mathrm{II}} &= (c_{13}A + c_{33})\left(\frac{\partial^3\psi}{\partial r^2\partial z} + \frac{1}{r}\frac{\partial^2\psi}{\partial r\partial z}\right) + c_{33}B\frac{\partial^3\psi}{\partial z^3} \\
\sigma_{rz}^{\mathrm{II}} &= c_{44}(A + B)\frac{\partial^3\psi}{\partial r\partial z^2} + \frac{\partial^3\psi}{\partial r^3} + \frac{1}{r}\frac{\partial^2\psi}{\partial r^2} - \frac{1}{r^2}\frac{\partial\psi}{\partial r}
\end{aligned} \tag{22}$$

Hence the problem is reduced to the determination of stress function ψ through the boundary conditions (14) and (8), which will be detailed in the next section.

3.2. Solution of sub-problem II

The function ψ can be assumed as

$$\psi = 2pa^3\int_0^\infty \left[\rho(k)I_0\left(k\sqrt{\lambda_1}\frac{r}{a}\right) + I_0\left(k\sqrt{\lambda_2}\frac{r}{a}\right)\right]f(k)\sin\frac{kz}{a}\sin\frac{kl}{2a}\,\mathrm{d}k \tag{23}$$

where I_0 is the zero-order modified Bessel function of the first kind, $\rho(k)$ and $f(k)$ are functions which will be determined later, λ_1 and λ_2 are given by (19). It is easy to verify that this assumed form of function ψ satisfies Eq. (18). The corresponding displacements and stresses can be obtained from (16) and (22) as follows:

$$\begin{aligned}
u_r^{\mathrm{II}} &= 2pa\int_0^\infty A\left[\sqrt{\lambda_1}\rho(k)I_1\left(k\sqrt{\lambda_1}\frac{r}{a}\right) + \sqrt{\lambda_2}I_1\left(k\sqrt{\lambda_2}\frac{r}{a}\right)\right]f(k)k^2\cos\frac{kz}{a}\sin\frac{kl}{2a}\,\mathrm{d}k \\
u_z^{\mathrm{II}} &= 2pa\int_0^\infty \left[(\lambda_1 - B)\rho(k)I_0\left(k\sqrt{\lambda_1}\frac{r}{a}\right) + (\lambda_2 - B)I_0\left(k\sqrt{\lambda_2}\frac{r}{a}\right)\right]f(k)k^2\sin\frac{kz}{a}\sin\frac{kl}{2a}\,\mathrm{d}k
\end{aligned} \tag{24}$$

$$
\begin{aligned}
\sigma_r^{\mathrm{II}} &= 2p\int_0^\infty \Big\{[(c_{11}A+c_{13})\lambda_1 - c_{13}B]\rho(k)I_0\Big(k\sqrt{\lambda_1}\frac{r}{a}\Big) + [(c_{11}A+c_{13})\lambda_2 - c_{13}B]I_0\Big(k\sqrt{\lambda_2}\frac{r}{a}\Big) \\
&\quad + (c_{12}-c_{11})\frac{Aa}{kr}\Big[\sqrt{\lambda_1}\rho(k)I_1\Big(k\sqrt{\lambda_1}\frac{r}{a}\Big) + \sqrt{\lambda_2}I_1\Big(k\sqrt{\lambda_2}\frac{r}{a}\Big)\Big]\Big\}f(k)k^3\cos\frac{kz}{a}\sin\frac{kl}{2a}\,\mathrm{d}k \\
\sigma_\theta^{\mathrm{II}} &= 2p\int_0^\infty \Big\{[(c_{12}A+c_{13})\lambda_1 - c_{13}B]\rho(k)I_0\Big(k\sqrt{\lambda_1}\frac{r}{a}\Big) + [(c_{12}A+c_{13})\lambda_2 - c_{13}B]I_0\Big(k\sqrt{\lambda_2}\frac{r}{a}\Big) \\
&\quad - (c_{12}-c_{11})\frac{Aa}{kr}\Big[\sqrt{\lambda_1}\rho(k)I_1\Big(k\sqrt{\lambda_1}\frac{r}{a}\Big) + \sqrt{\lambda_2}I_1\Big(k\sqrt{\lambda_2}\frac{r}{a}\Big)\Big]\Big\}f(k)k^3\cos\frac{kz}{a}\sin\frac{kl}{2a}\,\mathrm{d}k \\
\sigma_z^{\mathrm{II}} &= 2p\int_0^\infty \Big\{[(c_{13}A+c_{33})\lambda_1 - c_{33}B]\rho(k)I_0\Big(k\sqrt{\lambda_1}\frac{r}{a}\Big) \\
&\quad + [(c_{13}A+c_{33})\lambda_2 - c_{33}B]I_0\Big(k\sqrt{\lambda_2}\frac{r}{a}\Big)\Big\}f(k)k^3\cos\frac{kz}{a}\sin\frac{kl}{2a}\,\mathrm{d}k \\
\sigma_{rz}^{\mathrm{II}} &= 2pc_{44}\int_0^\infty \Big\{(\lambda_1 - A - B)\sqrt{\lambda_1}\rho(k)I_1\Big(k\sqrt{\lambda_1}\frac{r}{a}\Big) \\
&\quad + (\lambda_2 - A - B)\sqrt{\lambda_2}I_1\Big(k\sqrt{\lambda_2}\frac{r}{a}\Big)\Big\}f(k)k^3\sin\frac{kz}{a}\sin\frac{kl}{2a}\,\mathrm{d}k
\end{aligned}
\tag{25}
$$

In order to satisfy boundary condition (14), functions $\rho(k)$ and $f(k)$ are found to be

$$
\rho(k) = -\frac{(\lambda_2 - A - B)\sqrt{\lambda_2}I_1(k\sqrt{\lambda_2})}{(\lambda_1 - A - B)\sqrt{\lambda_1}I_1(k\sqrt{\lambda_1})} \tag{26}
$$

$$
\begin{aligned}
f(k) = -\frac{1}{\pi k^4}\Big\{&[(c_{11}A+c_{13})\lambda_1 - c_{13}B]\rho(k)I_0\Big(k\sqrt{\lambda_1}\Big) + [(c_{11}A+c_{13})\lambda_2 - c_{13}B]I_0\Big(k\sqrt{\lambda_2}\Big) \\
&+ (c_{12}-c_{11})\frac{A}{k}\Big[\sqrt{\lambda_1}\rho(k)I_1\Big(k\sqrt{\lambda_1}\Big) + \sqrt{\lambda_2}I_1\Big(k\sqrt{\lambda_2}\Big)\Big]\Big\}^{-1}
\end{aligned}
\tag{27}
$$

In the derivation of (27), we have used the following formula:

$$
\int_0^\infty \frac{1}{k}\cos\frac{kz}{a}\sin\frac{kl}{2a}\,\mathrm{d}k = \begin{cases} \dfrac{\pi}{2} & \text{for } |z| < \dfrac{l}{2} \\ 0 & \text{for } |z| > \dfrac{l}{2} \end{cases} \tag{28}
$$

$\rho(k)$ can be shown to have another form of expression,

$$
\rho(k) = -\frac{[(c_{13}A+c_{33})\lambda_2 - c_{33}B]\sqrt{\lambda_1}I_1(k\sqrt{\lambda_2})}{[(c_{13}A+c_{33})\lambda_1 - c_{33}B]\sqrt{\lambda_2}I_1(k\sqrt{\lambda_1})} \tag{29}
$$

It is therefore easy to check by using (29) or (26) that σ_z^{II} and $\sigma_{rz}^{\mathrm{II}}$ satisfy the stress-free boundary conditions at infinity in the sense of Saint-Venant principle, i.e., $\int_s \sigma_z^{\mathrm{II}}\,\mathrm{d}s = 0$ and $\int_s \sigma_{rz}^{\mathrm{II}}\,\mathrm{d}s = 0$, where s denotes the circular cross section of the rod.

3.3. Elastic strain energy

The total solution of the original problem is obtained from (9) by superposing the solutions of subproblems *I* and *II*. The total elastic strain energy W of the rod can be given as (Mura, 1987)

$$W = \frac{1}{2}\int_V \sigma_{ij}\varepsilon_{ij}^{e}\,\mathrm{d}V = -\frac{1}{2}[(\overline{\sigma_r}+\overline{\sigma_\theta})\varepsilon_1^* + \overline{\sigma_z}\varepsilon_2^*]V_\Omega \tag{30}$$

where V is the entire domain of the rod and V_Ω represents the volume of the inclusion ($V_\Omega = \pi a^2 l$); ε_{ij}^e is the elastic strain, $\overline{\sigma_r}$, $\overline{\sigma_\theta}$ and $\overline{\sigma_z}$ denote the average of stresses σ_r, σ_θ and σ_z over the inclusion Ω:

$$\overline{\sigma_r} = \frac{1}{V_\Omega}\int_\Omega \sigma_r\,\mathrm{d}V \quad \overline{\sigma_\theta} = \frac{1}{V_\Omega}\int_\Omega \sigma_\theta\,\mathrm{d}V \quad \overline{\sigma_z} = \frac{1}{V_\Omega}\int_\Omega \sigma_z\,\mathrm{d}V \tag{31}$$

From our above solution it is easy to show that

$$\begin{aligned}&\overline{\sigma_r}+\overline{\sigma_\theta} = -2\left(c_{11}+c_{12}-\frac{2c_{13}^2}{c_{33}}\right)\varepsilon_1^* H\left(\frac{l}{a}\right)\\ &\overline{\sigma_z} = 0\end{aligned} \tag{32}$$

with

$$H\left(\frac{l}{a}\right) = 1 + \frac{4a}{l}\int_0^\infty k f(k) g(k)\left(\sin\frac{kl}{2a}\right)^2 \mathrm{d}k \tag{33}$$

where $f(k)$ is given in (27) and

$$\begin{aligned}g(k) = {} & \frac{[(c_{11}A+c_{13})\lambda_1 - c_{13}B]}{\sqrt{\lambda_1}}\rho(k) I_1\left(k\sqrt{\lambda_1}\right) + \frac{[(c_{11}A+c_{13})\lambda_2 - c_{13}B]}{\sqrt{\lambda_2}} I_1\left(k\sqrt{\lambda_2}\right)\\ & + \frac{[(c_{12}A+c_{13})\lambda_1 - c_{13}B]}{\sqrt{\lambda_1}}\rho(k) I_1\left(k\sqrt{\lambda_1}\right) + \frac{[(c_{12}A+c_{13})\lambda_2 - c_{13}B]}{\sqrt{\lambda_2}} I_1\left(k\sqrt{\lambda_2}\right)\end{aligned} \tag{34}$$

Hence the elastic strain energy of the rod can be obtained as

$$W = \left(c_{11}+c_{12}-\frac{2c_{13}^2}{c_{33}}\right)(\varepsilon_1^*)^2 H\left(\frac{l}{a}\right) V_\Omega \tag{35}$$

where $V_\Omega = \pi a^2 l$ is the volume of the inclusion. Since the elastic strain energy is always positive, it requires that $c_{11}+c_{12}-2c_{13}^2/c_{33} > 0$, which is also the condition for a tensile lateral pressure given by (14) and (15). One can see from (35) that $H(l/a)$ serves as the shape factor of the cylindrical inclusion in the rod. In fact, $H(l/a)$ plays the similar role as the Eshelby's tensor S_{ijkl} for ellipsoidal inclusions (Eshelby, 1957). For given a, ε_1^*, c_{11}, c_{12}, c_{13}, c_{33} and c_{44}, W is a function of l only.

4. Discussions and examples

Some characteristics of the solution can be observed, as follows:

(1) It should be noted that the derived solution for the transversely isotropic case does not apply for the isotropic case due to the degeneracy of the Bessel functions. For isotropic cases, $\lambda_1 = \lambda_2 = 1$, and the two Bessel function terms become degenerate. Accordingly, the expressions, (24), (25) and (30), of displacements, stresses and elastic strain energy are not valid for isotropic cases. The solution for the isotropic case is to add a new Bessel function term that depends on $I_1(kr/a)$ in the function ψ. The detail derivation of the solution of the isotropic case has been given in our previous paper (Zhong et al., 2000).

(2) We have pointed out in Section 3.1 that p_1 and p_2 are either real or complex. When p_1 and p_2 are complex they are complex conjugates. By inspection of expressions (24), (25) and (30), and resolving all

complex terms into their real and imaginary parts, it can be found that the imaginary parts are totally cancelled each other and only the real parts are left. Therefore, the obtained displacements, stresses and elastic strain energy are real.

(3) The axial component of eigenstrain ε_z^* has no contribution to the stresses and the total elastic strain energy of the rod. It induces only an axial displacement of the rod.

(4) It should be noted that the inclusion-matrix system developed in this paper is a simplified model with several assumptions. For example, the inclusion is assumed to have the same elastic properties as the matrix, but the martensite and austenite phases in a real SMA are known to have different elastic moduli. Also, the assumed planar interface between phases is a rather strong constraint of the kinematics across a transformation front. Other morphologies of the interface might be energetically more favorable. These factors must be further incorporated into the model if a quantitative comparison with the test data of a real SAM is to be made.

As an example, we consider the case with $c_{12}/c_{11} = c_{13}/c_{11} = 3/7$, $c_{44}/c_{11} = 2/7$ and $c_{33}/c_{11} = 0.5, 1.5, 2$. Figs. 3 and 4 show the variation of stresses σ_r and σ_z (normalized by $c_{11}\varepsilon_1^*$) along the positive z-axis (for $r = 0$, $z \geqslant 0$, we have $\sigma_r = \sigma_\theta$ and $\tau_{zr} = 0$) for $l/a = 10$. In the figures the case of an isotropic material ($c_{12}/c_{11} = c_{13}/c_{11} = 3/7$, $c_{44}/c_{11} = 2/7$ and $c_{33}/c_{11} = 1$) is also depicted based on the solution obtained by Zhong et al. (2000). It can be observed that both σ_r and σ_z concentrate near the inclusion-matrix interface ($z = 5a$) and decrease rapidly to zero away from the interface. The stress σ_r has a jump across the interface while σ_z is still continuous across the interface. The greater c_{33}/c_{11} value, the higher the stress concentration near the interface. This means that the stiffening of the rod along the longitudinal direction or the softening in the transversal direction will increase the stress concentrations. There is almost no interaction between the stress fields of the two neighboring interfaces for the considered case $l/a = 10$. However, when the two

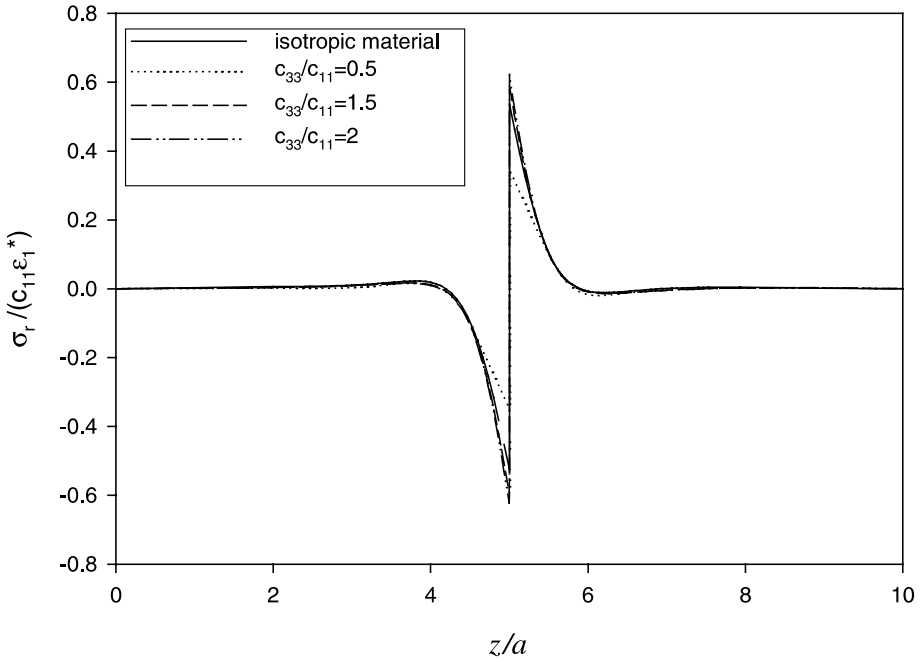

Fig. 3. The variation of stresses σ_r normalized by $c_{11}\varepsilon_1^*$ along the positive z-axis when $l = 10a$.

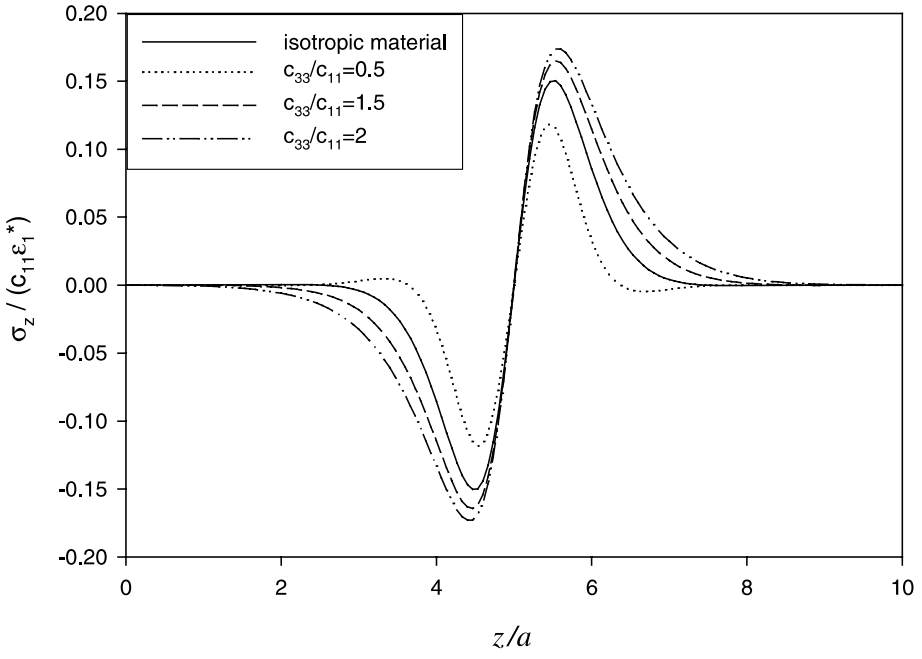

Fig. 4. The variation of stresses σ_z normalized by $c_{11}\varepsilon_1^*$ along the positive z-axis when $l = 10a$.

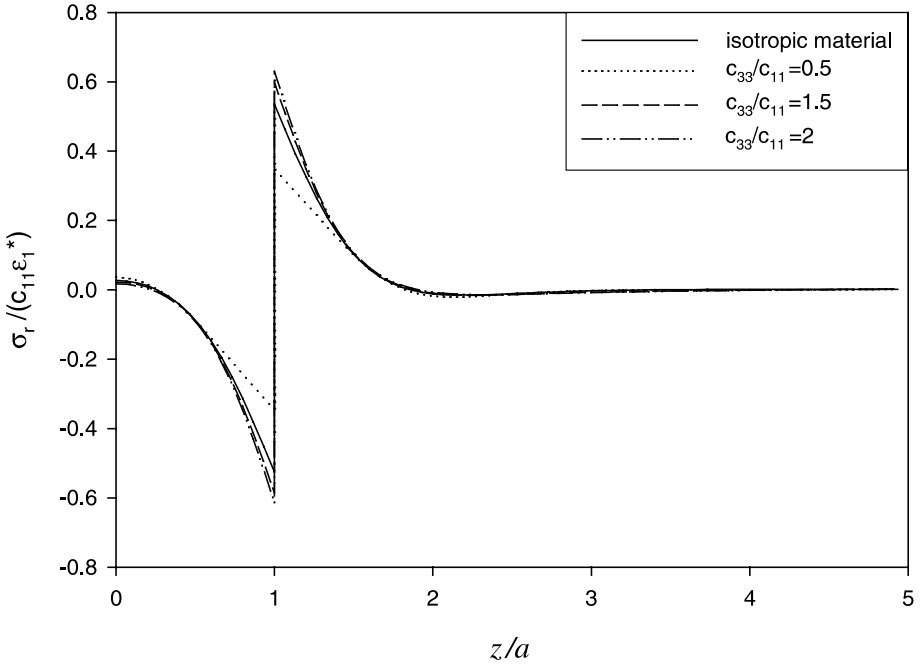

Fig. 5. The variation of stresses σ_r normalized by $c_{11}\varepsilon_1^*$ along the positive z-axis when $l = 2a$.

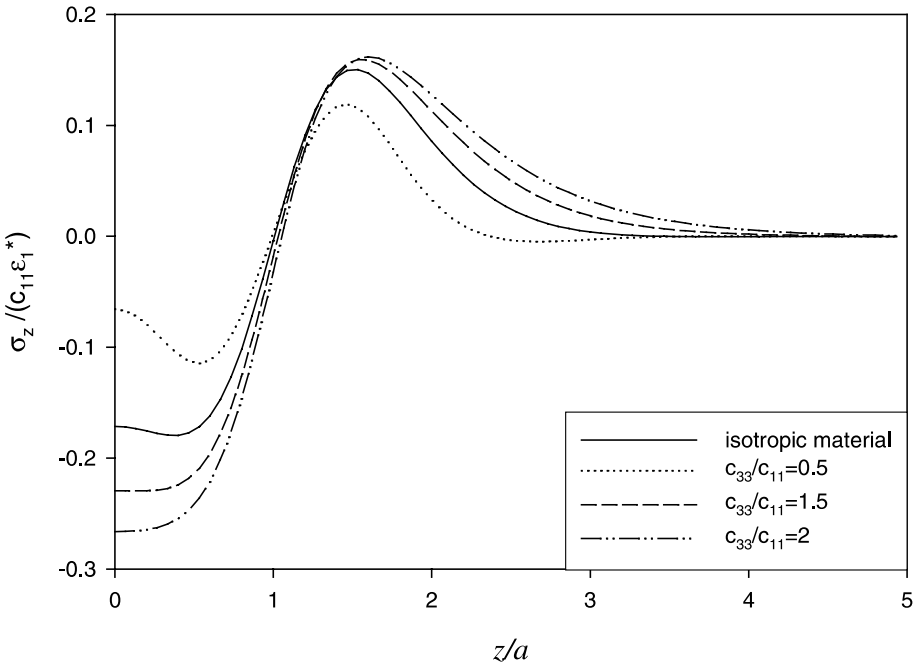

Fig. 6. The variation of stresses σ_z normalized by $c_{11}\varepsilon_1^*$ along the positive z-axis when $l = 2a$.

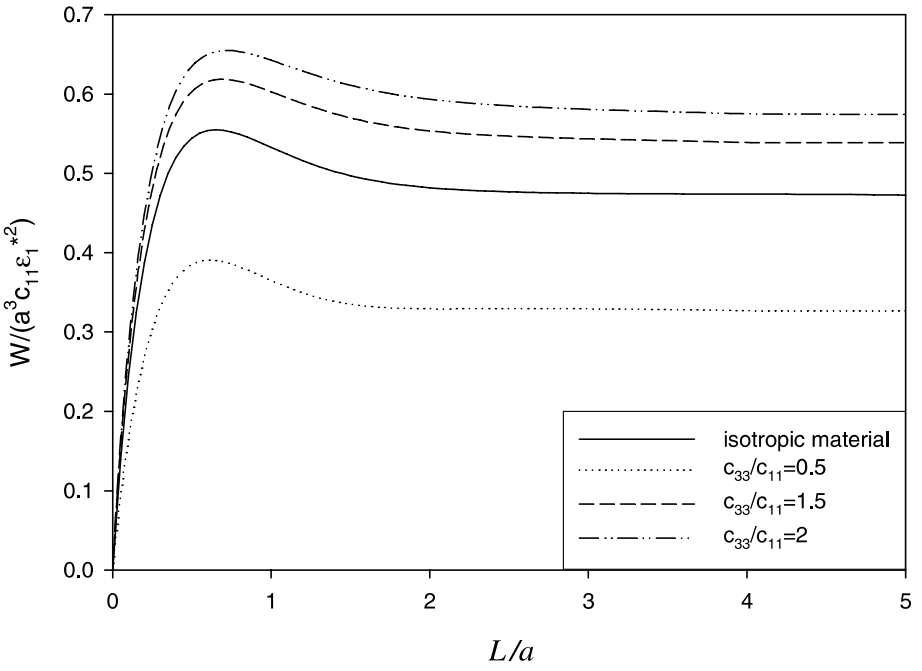

Fig. 7. The variation of the elastic strain energy W (normalized by $a^3c_{11}\varepsilon_1^{*2}$) of the rod as a function of the normalized length of the inclusion l/a.

interfaces come closer, the interaction of the stress fields of the neighboring interfaces becomes obvious. This phenomenon can be observed in Figs. 5 and 6 which show the variation of stresses σ_r and σ_z (normalized by $c_{11}\varepsilon_1^*$) along the positive z-axis ($r = 0, z \geqslant 0$) for $l/a = 2$. It is seen that the stresses in the center region of the inclusion do not vanish due to the interaction of the interfaces, and the stress concentration increases as the two interfaces approach each other. Fig. 7 shows the variation of the elastic strain energy W (normalized by $a^3c_{11}\varepsilon_1^{*2}$) of the rod as a function of the normalized length of the inclusion l/a for the same problem. The normalized elastic strain energy for an isotropic material ($c_{12}/c_{11} = c_{13}/c_{11} = 3/7, c_{44}/c_{11} = 2/7$ and $c_{33}/c_{11} = 1$) is also calculated based on the solution by Zhong et al. (2000) and depicted in the same figure. Several typical features of the normalized elastic strain energy can be identified. The normalized elastic strain energy increases monotonically and reaches a peak value as the inclusion grows. Further growth of the inclusion causes a decrease in the elastic strain energy and very quickly approaches a steady value. The normalized elastic strain energy increases with the increase of the ratio c_{33}/c_{11}. This reveals that the rod will have higher elastic strain energy if the rod is stiffer along the longitudinal direction or softer in the transversal direction.

5. Summary

An analytical solution is obtained for the axisymmetric deformation of a transversely isotropic rod containing a single cylindrical inclusion with uniform eigenstrains by means of the principle of superposition. The original problem is divided into two sub-problems to derive the analytical expressions for the displacements, stresses and elastic strain energy of the rod. The effects of microstructural parameters and its evolution on the elastic stress and strain fields as well as the strain energy of the rod are quantitatively demonstrated through examples. The results show that the stiffening of the rod along the longitudinal direction or the softening in the transversal direction will increase the stress concentrations near the interface between the inclusion and the matrix. It also reveals that the rod will have higher elastic strain energy if the rod is stiffer along the longitudinal direction or softer in the transversal direction.

Acknowledgements

The reported work was performed with the financial support of the National Natural Science Foundation of China, the National Excellent Young Scholar Foundation of China, the Teaching and Research Award Fund for Outstanding Young Teachers in High Education Institutions of MOE, PRC and the Research Grant Council of Hong Kong SAR of China (PolyU 1/99C).

References

Eshelby, J.D., 1957. The determination of the elastic field of an ellipsoidal inclusion and related problems. Proceedings of the Royal Society A 241, 376–396.

Lekhnitski, S.G., 1981. Theory of an Anisotropic Body. MIR Publishers, Moscow.

Leo, P.H., Shield, T.W., Bruno, O.P., 1993. Transient heat transfer effects on the pseudoelastic behavior of shape-memory wires. Acta Metallurgica 41, 2477–2485.

Lin, P.H., Tobushi, H., Tanaka, K., Hattori, T., Makita, M., 1994. Pseudoelastic behaviour of TiNi shape memory alloy subjected to strain variations. Journal of Intelligent Material Systems and Structures 5, 694–701.

Mura, T., 1987. Micromechanics of Defects in Solids, second ed. Martinus Nijhoff Publishers.

Shaw, J.A., Kyriakides, S., 1995. Thermomechanical aspects of NiTi. Journal of the Mechanics and Physics of Solids 43, 1243–1281.

Shaw, J.A., Kyriakides, S., 1997. On the nucleation and propagation of phase transformation fronts in a NiTi alloy. Acta materialia 45, 683–700.

Sun, Q.P., Zhong, Z., 2000. An inclusion theory for the propagation of martensite band in shape memory alloy wire under tension. International Journal of Plasticity 16, 1169–1187.

Zhong, Z., Sun, Q.P., Tong, P., 2000. On the axisymmetric deformation of a rod containing a single cylindrical inclusion. International Journal of Solids and Structure 37, 5943–5955.